

## QUALITY OF WATER VAPOUR WINDS

A. Eriksson  
Freie Universität Berlin  
Federal Republic of Germany

Abstract: The current methods of WV-channel wind tracking are reviewed. While Water Vapour Winds (WVW) interactively derived from GOES-VAS sequences prove to be of the same quality as IR-channel cloud track winds, development of tracking algorithms for METEOSAT WVW was slowed down due to the unfavourable noise structure of the METEOSAT2 WV imagery. With METEOSAT3 the quality of the WV imagery raised considerably, so that, in future, more use should be made of its dynamic information content.

Interactively derived WVW inherit a subjective component, since it is, for most cases, not possible to apply cross-correlation techniques to amorphous WV structures. A new, differential approach for automated computation of displacement vector fields from local grey value variations in image sequences is presented, together with test results for METEOSAT2 and METEOSAT3 WV imagery. While some of these purely automatically derived vector fields already were in good agreement with interpolated RAWIN fields or MIEC cloud track winds and ECMWF twelve-hourly forecasts, others exhibited, at least in parts, lack of any relevant information.

### 1. INTRODUCTION

For several years, channels in the water vapour absorption band have been included onboard METEOSAT (6.3 $\mu$ m) and GOES (6.7 $\mu$ m and 7.2 $\mu$ m) satellites. The imagery in the WV channel represents the tropospheric water vapour content above 600hPa, with maxima of the contribution function at about 550hPa-450hPa for cloud free areas (Poc et. al., 1980). Dark areas represent a dry upper troposphere with higher radiances stemming from relatively low levels, while white areas represent a wet upper troposphere

with accordingly low radiances. High clouds with their corresponding low radiances can clearly be detected in the WV channel as well.

Animated sequences of WV images give, due to the continuity in time and space of the WV features, an insight in the dynamics of the middle and upper troposphere (Morel et.al., 1978). The continuity of the WV structures makes them attractive for deriving motion information from satellite sequences in areas, where due to a lack of medium and high level clouds it cannot be obtained by usual Cloud Track Winds (CTW). On the other hand it is just the continuous and fuzzy structure that makes application of commonly applied tracking methods, especially cross-correlation methods, difficult for the WV channel.

The feasibility of tracking water vapour structures in consecutive images to derive mid-tropospheric winds has already been demonstrated by Kästner et.al. (1980) with overlapping passes of NIMBUS5 THIR data in the  $6.3\mu\text{m}$  channel. Eigenwillig and Fischer (1982) demonstrated by manually tracking "pure" water vapour structures in METEOSAT1 images that an accuracy comparable to CTW can be achieved. When applying their techniques to METEOSAT2 imagery they failed due to its unfavourable noise structure (Gesell et.al., 1984; Fischer et.al., 1987). Stewart et.al. (1985) reported RMS vector differences of 8m/s for both cloud and water vapour features tracked in GOES-VAS  $6.7\mu\text{m}$  imagery.

Despite these encouraging results, until now, to the knowledge of the author, no WWV have been produced on an operational basis. Main reasons for this may be that so far, only techniques where the operator marks start and end positions of selected targets in consecutive images have been proven to provide results of sufficient accuracy. These methods do not only result in a high time consumption, but also introduce a "subjective factor".

## 2. TRACKING TECHNIQUES WITH OPERATOR SELECTED TARGETS

The techniques have been adopted from interactive tracking algorithms for CTW. In a sequence of consecutive satellite images, typically three, the operator selects an appropriate structure drifting with the wind. The position of the structure

is determined in consecutive images, either by manual selection by the operator (single point tracking), or by some kind of correlation technique (mostly cross-correlation). Knowing the geographical positions of tracked objects in both images and the time interval separating the images, a displacement vector can be computed.

## 2.1 Selection of targets

In order to derive actually mid- or high-tropospheric winds from the WV channel, only features drifting with the wind should be tracked and then be assigned to an appropriate atmospheric level. The fuzzy nature of WV structures makes them a generally difficult target for tracking. This difficulty is even enhanced by the quality of WV imagery available: in case of VAS data because of the poor horizontal resolution of 16km; in case of METEOSAT1 and METEOSAT2 because of the severe corruption by noise. For METEOSAT3 the quality of the WV imagery has improved considerably, so that in future it should be easier to identify suitable structures for tracking.

The approach of Eigenwillig and Fischer (1982) was to select only "pure" water vapour structures as targets, which they defined as discontinuities separating darker from brighter areas. The idea was that these mid-tropospheric winds should supplement usual CTW in areas where, due to the absence of relevant clouds, no mid- or high-tropospheric winds could be derived. In order to enhance these "pure" WV structures, different filter techniques had to be applied to the METEOSAT WV scenes (Eigenwillig and Fischer (1982), Gesell et. al. (1984)). Despite the enhancements applied, the structures to be tracked were not defined clearly enough to serve as tracers for cross-correlation techniques. In a later study Fischer et.al. (1987) also reported the successful computation of a few WVV employing cross-correlation techniques when applying strong quality checks.

In contrast to Fischer, Stewart et.al. (1985) tracked both clouds and WV inhomogeneities in consecutive VAS 6.7 $\mu$ m images without prior enhancement of WV structures by sophisticated combinations of filters. In this way they were able to derive dense vector fields with uniform coverage and high accuracy

over the United States. Again, cross-correlation techniques proved to be inadequate for tracking.

## 2.2 Height assignment

Stewart et.al. (1985) assigned altitude to the  $6.7\mu\text{m}$  WVW by the level where brightness temperature equalled actual air temperature. With this approach, RMS vector differences between WVW and co-located radiosonde winds could be reduced from 8.8m/s, at a mandatory 400hPa level, to only 7.9m/s at the assigned level. A later study of Hayden et.al. (1987) reported for both, level of best fit (LBF) and assigned level, a mean height assignment to approximately 300hPa for the  $6.7\mu\text{m}$  WVW, while newly introduced  $7.2\mu\text{m}$  winds were in the average assigned to about 400hPa.

For METEOSAT ( $5.7\mu\text{m}$ - $7.1\mu\text{m}$ ) Fischer et.al.(1981) studied the variability of the distribution function with atmospheric temperature and humidity profiles and the satellite viewing angle. They found a minor sensitivity to changes in the temperature profile, but a pronounced dependence on humidity profiles and viewing angle. The half width center of the contribution function was reported to lie between 560hPa and 360hPa and the major contributing layer to be about 320hPa thick. According to their results, they compared the "pure" WVW with co-located radiosondes at 400hPa and 500hPa and found a better agreement with the 400hPa assignment. In a later report Fischer et.al. (1987) used a radiative transfer model in combination with actual temperature and humidity profiles for height assignment. They reported height assignments mainly between 400hPa to 500hPa. However, their method of height assignment is only applicable to cloud free regions.

## 2.3 Quality of products

A comparison of VAS  $6.7\mu\text{m}$  WVW, VAS  $7.2\mu\text{m}$  WVW and METEOSAT1  $6.3\mu\text{m}$  WVW with co-located radiosondes is presented in Tab. 1. For comparison, GOES and METEOSAT cloud track winds for high levels are included as well. WVW derived by single point tracking show a comparable quality to usual CTW. To appreciate the high accuracy of WVW, one should also keep in mind that before 1984 accuracies of CTW were typically in the order of 10-11m/s.

	RMS vect.diff. in m/s	pressure level in hPa	No. of comp.
VAS 6.7 $\mu$ m (*)	8.3	305(mean)	187
VAS 7.2 $\mu$ m (*)	9.1	395(mean)	210
VAS 6.7 $\mu$ m (**)	8.8	400	2023
Meteosat1 WV (+)	4.9	400	87
GOES IR (*)	8.3	<400	
METEOSAT IR (*)	9.8	<400	

Tab. 1: Comparison of WVW and CTW with co-located RAWIN.  
 ((\*) Hayden et.al. (1987), (\*\*) Stewart and Hayden  
 (1985), (+) Eigenwillig and Fisher (1982))

### 3. APPROACHES TO AUTOMATED WVW TRACKING

Some general remarks about the special nature of the WV channel should precede detailed discussion. Fischer et.al. (1987) as well as Stewart et.al. (1985) have stated that preferably single point tracking by an experienced operator should be used to derive WVW. This approach offers two principal advantages over automated (cross-correlation) techniques:

- Due to the amorphous WV structures it is difficult to detect and follow defined targets objectively. The human operator is helped by his ability to visually integrate conceivable motions in animated image sequences (Warnecke, 1983).
- Not all displacements detectable in the WV channel represent a "wind" at a certain level of the atmosphere. Some of the apparent displacements may be more linked to the propagation of weather systems of different scales (Desbois et.al., 1988). To really determine wind speeds, it should, for example, be avoided to track convective complexes and any phenomena in areas of strong vertical wind shear. In contrast to automated systems, a skilled operator can restrict wind computation to reliable targets from the beginning.

#### 3.1 Monthly displacement vector fields from ISCCP WV data

In order to obtain monthly averaged displacement vector fields over Afrika, Desbois et.al. (1988) calculated displacement vector fields from ISCCP B2 pictures in the WV channel. The spacial resolution of the data is reduced to approximately 30km while the time resolution is reduced to three hours. An

automatic cross-correlation technique was applied to appropriately filtered images. The subsequent automated quality control was performed by allowing only vectors with a high correlation coefficient. Undetected "false" drift vectors were assumed to be randomly distributed in speed and direction and thus would, after monthly averaging, only reduce the drift speed proportional to the amount of false vectors at a certain location. For the averaged vector fields, a qualitatively good agreement could be observed with conventional mean wind fields. In comparison with ECMWF analysis, some of the interannual variability of the upper tropospheric circulation was as well represented in the mean WV drift fields. Desbois et.al. stated, that more research has to be done in order to improve tracking algorithm, quality control and the interpretation of the resulting mean drift fields.

### 3.2 A new, differential approach to deriving displacement vector fields applied to METEOSAT WV imagery

For the automated computation of current WVW fields, one may employ vector computation algorithms, which try to imitate the capacity of the human eye to smoothly integrate movements in space, and thus try to quantitize the "optical flow" as defined by Horn and Schunck (1981).

For a couple of years new approaches of that kind have been discussed in the image processing literature. Approaches based on simple functional approximations of the local grey value variation, combined with assumptions about the general behaviour of the vector field, offer several advantages:

- They do not need an explicit definition of objects or structures like corners, edges, intensity peaks etc.
- They are capable of estimating a displacement vector for each pixel.
- They are accessible to analytical analysis (Nagel and Enkelmann, 1983).

An algorithm formulated by Nagel (1983c) and Enkelmann (1985) is here applied to METEOSAT2 and METEOSAT3 sequences in the water vapour channel.

### 3.2.1 Description of the algorithm

The grey value distribution in a small neighbourhood of a location  $\vec{x}$  can be described as a simple function of the coordinates in the image plane, for example by the first terms of a Taylor expansion. It is assumed, that the same functional description is also a valid approximation for the pixel corresponding to  $\vec{x}$  in the following image. This principle can be illustrated using a one-dimensional example (Fig. 1, from Nagel (1985)). It is assumed, that the image function  $g(x)$ , representing the grey value distribution, can be approximated by a linear function in the neighbourhood of  $x$ . The requirement that the grey value distribution at a given time  $t$  is identical with the one at  $t+\Delta t$  can be expressed differentially as

$$dg(x,t) = 0 = \frac{\partial g(x,t)}{\partial x} dx + \frac{\partial g(x,t)}{\partial t} dt \quad (1a)$$

$$0 = \frac{\partial g(x,t)}{\partial x} \frac{dx}{dt} + \frac{\partial g(x,t)}{\partial t} = g_x u + g_t \quad (1b)$$

(partial derivatives denoted by subscript)

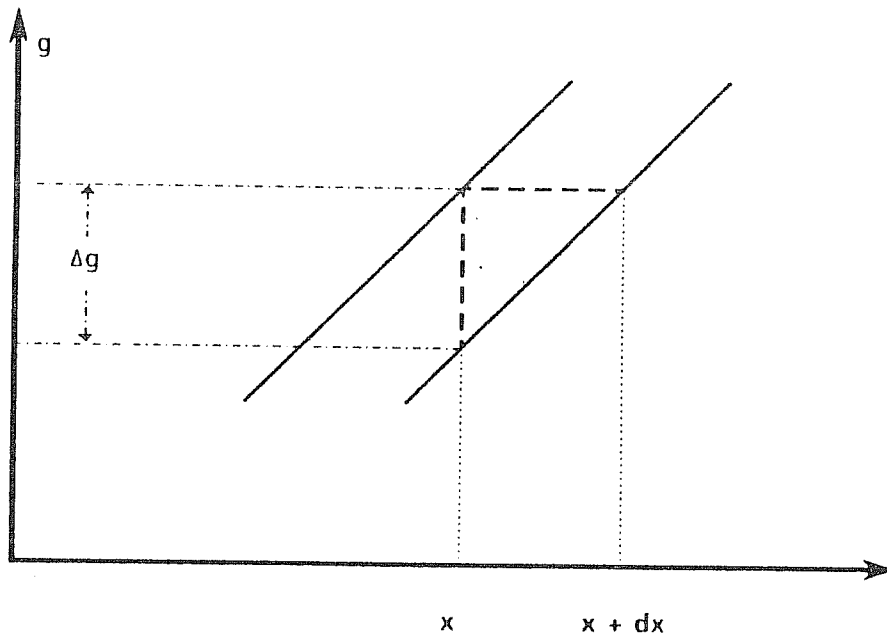


Fig.1: For a linear one-dimensional function  $g(x)$ , which is displaced parallel to itself, the displacement  $u=dx$  can be calculated from the grey value difference  $\Delta g$  and the slope of the function  $g(x)$

Thus for the one-dimensional linear case the displacement can be written as

$$u = - \frac{g_t}{g_x} \quad (2)$$

For the two-dimensional image plane a location is given by a vector  $\vec{x}=(x,y)$ , the image function by  $g=g(x,y,t)$ . Analog to (1) it can be derived for the linear case

$$0 = g_x u + g_y v + g_t \quad (3)$$

Here a principle difficulty arises: only one relation between the components  $u$  and  $v$  of the displacement vector  $\vec{u}=(u,v)^T$  is given by (3) (namely the component in the direction of the grey value gradient).

For a realistic modelling of an image function in the two-dimensional case also second order derivatives of the image function, describing the change of the grey value gradient, have to be considered. That way, enough information can be provided at grey value corners to calculate both components of the displacement vector (Nagel, 1983a).

To estimate displacement vectors in areas, where the mere grey value variation is not sufficient to estimate both components of the vector, realistic assumptions about the general behaviour of the vector field have to be added.

A plausible assumption about the behaviour of the vector field was formulated by Horn and Schunck (1981): the vector field shall only vary smoothly as a function of image position. This requirement allows the displacement in an iterative process to travel into areas with a linear or partial homogeneous grey value distribution. The disadvantage of such a general requirement is, that real discontinuities in the vector field might get wiped out during the iterative process. Therefore the less general smoothness requirement of "oriented smoothness" was formulated by Nagel (1983c). He suggested that the weight given to the smoothness constraint should be directly influenced by the local grey value structure. Smoothness constraints should only be applied to areas where the local grey value distribu-



tion does not provide enough information to estimate both components of the displacement vector (like for example along grey value edges). In the direction of the grey value gradient, where enough information is provided and also real discontinuities could occur, the smoothness requirement should be suppressed. The actual effect of such a oriented smoothness requirement will be, that the smoothness constraint helps the displacement to propagate along grey value edges. This is an appropriate assumption for the WV channel, as shown by Allison et.al. (1972).

Nagel (1983c) formulated these requirements as a minimization problem:

$$\iint dx dy \{ (g_2(\vec{x}) - g_1(\vec{x} - \vec{u}))^2 + \alpha^2 \text{trace}((\nabla \vec{u})^T W (\nabla \vec{u})) \} \Rightarrow \min \quad (4)$$

The first term takes into account the displacement calculated from the mere grey value variation, the second term expresses the oriented smoothness requirement with W as a weight matrix. The system of nonlinear differential equations resulting from (4) is solved in an iterative multigrid algorithm (Enkelmann 1985).

### 3.2.2 Tests with METEOSAT WV data

In many cases, the fuzzy and continuously moving structures to be found in the water vapour channel seem to provide adequate targets for estimating displacement vectors with the new algorithm. A couple of strong and weak points of the algorithm could be identified when applying it to METEOSAT2 and METEOSAT3 WV sequences:

-In most cases, the main features of the mid- to upper-tropospheric flow were captured in the vector field. Nevertheless, there was always a considerable proportion of the vector field which obviously did not account to the actual atmospheric motion, and often could be attributed to one of the deficiencies in the algorithm or image data listed below.

- The system proved to be very sensitive regarding changes of size and shape of structures in the image sequence. Thus high clouds, especially when of convective nature, often lead to unrealistic displacement vectors.
- Large homogeneous areas can sometimes not be reached by the smoothness requirement. This results in very low wind speeds computed for these areas.
- Specially for METEOSAT2: local changes of noise structure from image to image may strongly influence the local displacement vectors. Nevertheless, with an implemented Gaussian filter the algorithm seems to be rather tolerant regarding the noise of METEOSAT2. Tests with visually better filters (lowpass filters with a filter radius depending on whether an edge was detected) only lead to slightly different results in these problem areas.
- METEOSAT3 shows a different noise structure from METEOSAT2, which in the special case of this algorithm seems to lead to even more serious problems. With the more systematic nature of the noise and the overall better image quality, it should, however, be possible to help this problem by applying appropriate filters.
- There are indications that the direction of the vector field might in some cases be forced by well defined high clouds, while the speed is more representative for the lower altitude structures in between.
- Quantitative reliability of displacement vectors calculated outside problem areas is proved by the fact, that they often show a nearly exact agreement in direction and speed with winds interactively derived with cross-correlation at well defined structures.

As in all automated systems, a quality control is necessary. Due to the large number of vectors calculated by the algorithm, (one vector per pixel or per square of 2\*2 pixels), at least the first steps of quality control have to be performed automatically.

Since most disturbances in the vector field do not carry any meteorological significance, we are, as a first step in quality

control, presently testing different internal consistency checks for the vector field. The schemes tested so far had in common, that they were checking for consistency with vectors in a certain neighbourhood. More work has to be done here, since a too high proportion of vectors with consistent behaviour on a larger scale is sorted out, while still small groups of obviously wrong vectors slip through the quality control.

For "good" vector fields, mean directional differences of  $40^{\circ}$ - $60^{\circ}$  compared to other data sources, typically reduce to  $20^{\circ}$ - $30^{\circ}$  when applying internal quality checks. After quality control RMS vector differences typically lie in the range of 8.5m/s-16m/s. The comparisons were either made with interactively derived CTW and interpolated RAWIN (for METEOSAT2), or to ECMWF 12-hourly forecasts and MIEC-CTW. When comparing to ECMWF and Rawin data, best agreement was found between 500hPa to 400hPa.

It has to be added, that some vector fields calculated from METEOSAT3 data did show no correspondence to the actual mid- or upper-tropospheric flow. Even without comparison to other data, the inferior quality of these vector fields was obvious. When applying internal quality controls to them, the resulting fields were very inconsistent. The reasons for these discrepancies are under investigation.

Some examples of derived vector fields are given in Fig. 2-8. Statistics for these fields, in comparison with those of CTW from 1979-1982 are given in Tab.2.

It can be stated that the vector computation algorithm in its current form still yields many problems when confronted with data as complex as WV imagery. Nevertheless, it could already be shown that for various cases accuracies comparable to those of CTW in the beginning of the 1980's could be reached.

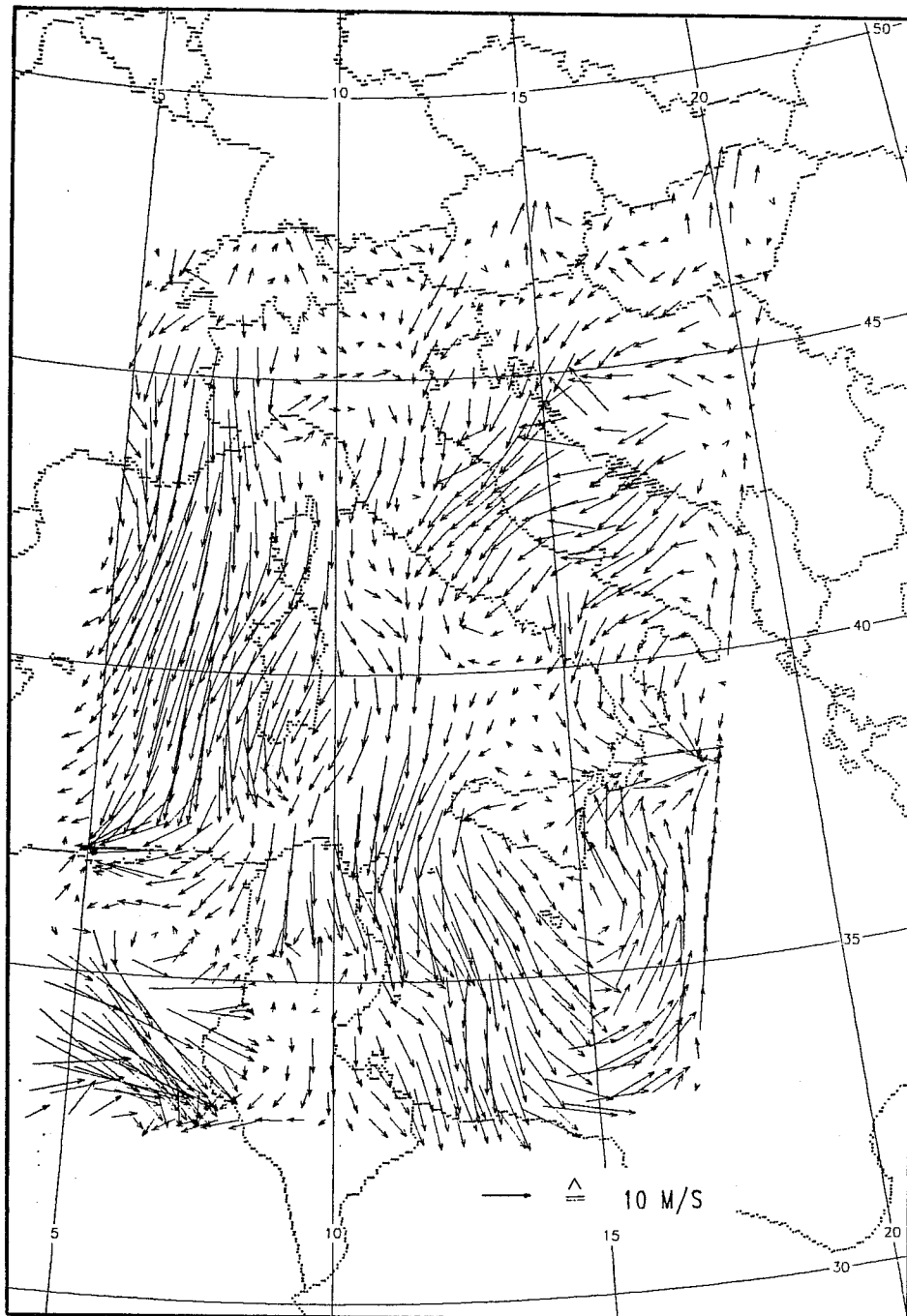


Fig. 2: Case 1: 27 FEB 1982, 11-12GMT, Mediterranean. METEOSAT2  
WV displacement vectors before quality control

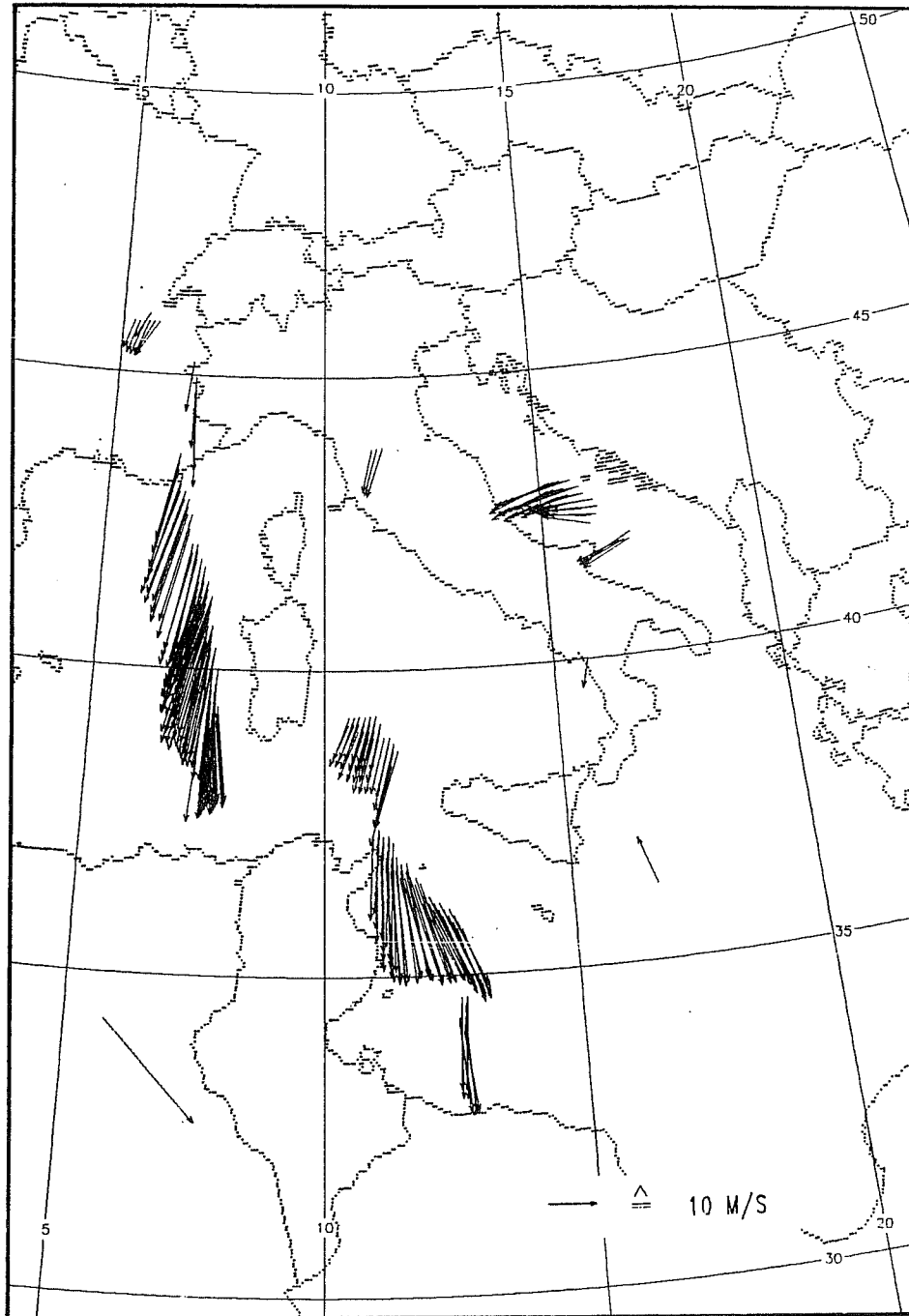


Fig. 3: Same as Fig.2, but after internal consistency checks

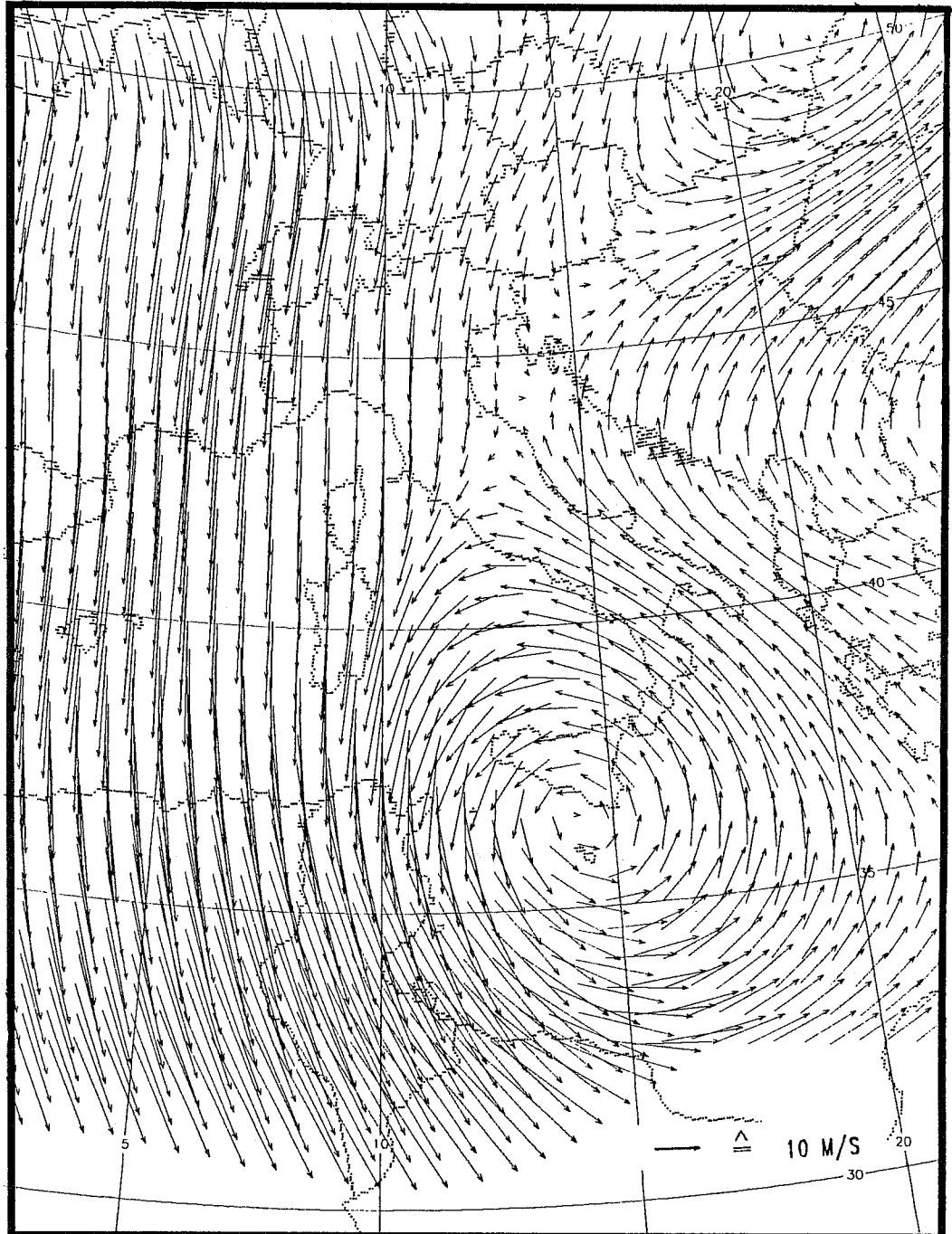


Fig. 4: Interpolated RAWIN field 500hPa for case 1  
27 FEB 1982, 12GMT

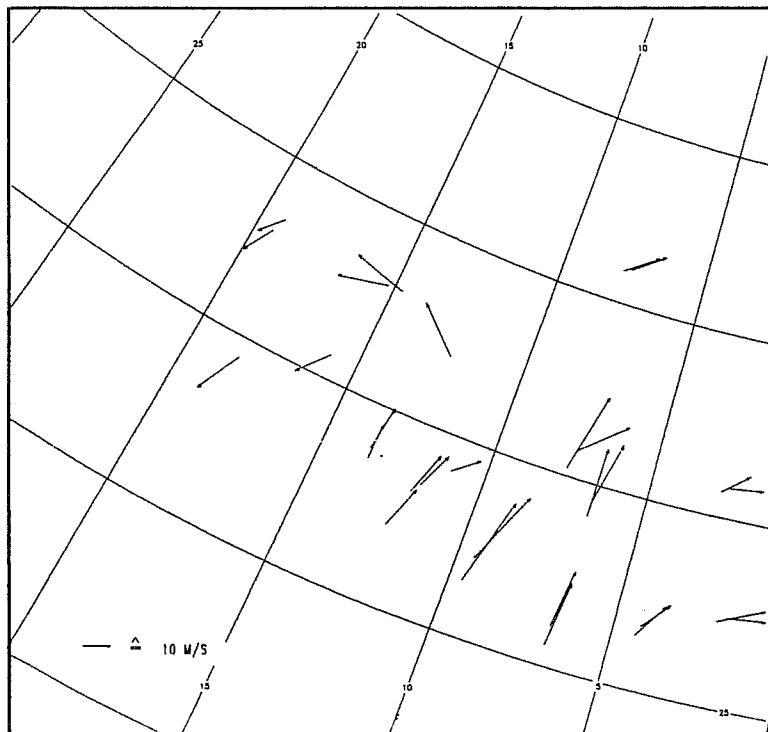
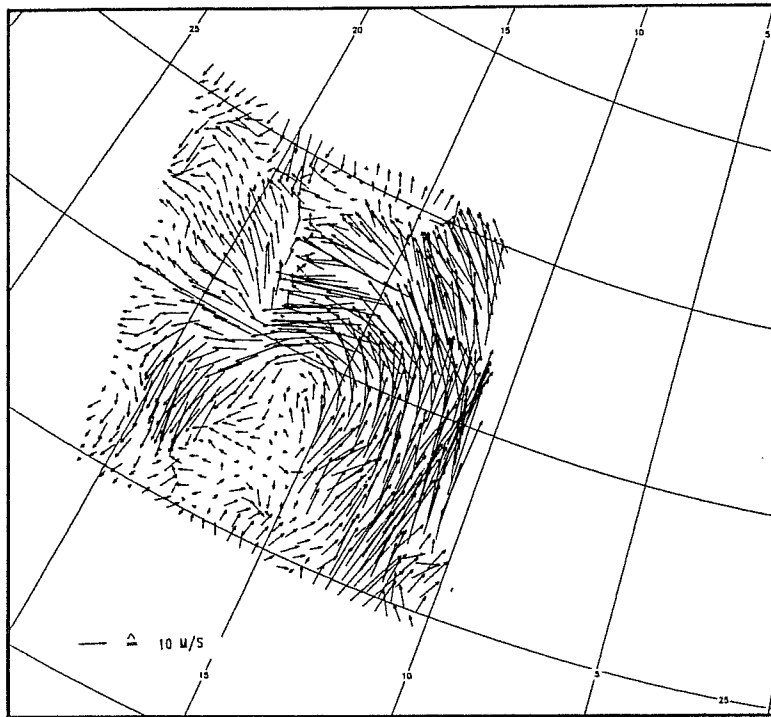


Fig. 5: Case 2: 20 SEPT 1984, 22.30-23.00GMT, eastern subtropical Atlantic Ocean (Canary Islands).  
 Upper: METEOSAT2 WV displacement vector field  
 Lower: interactively tracked IR-CTW in high and medium levels. Without performing a quality control, mean vector differences were 11.5m/s, the mean directional difference was 32°.

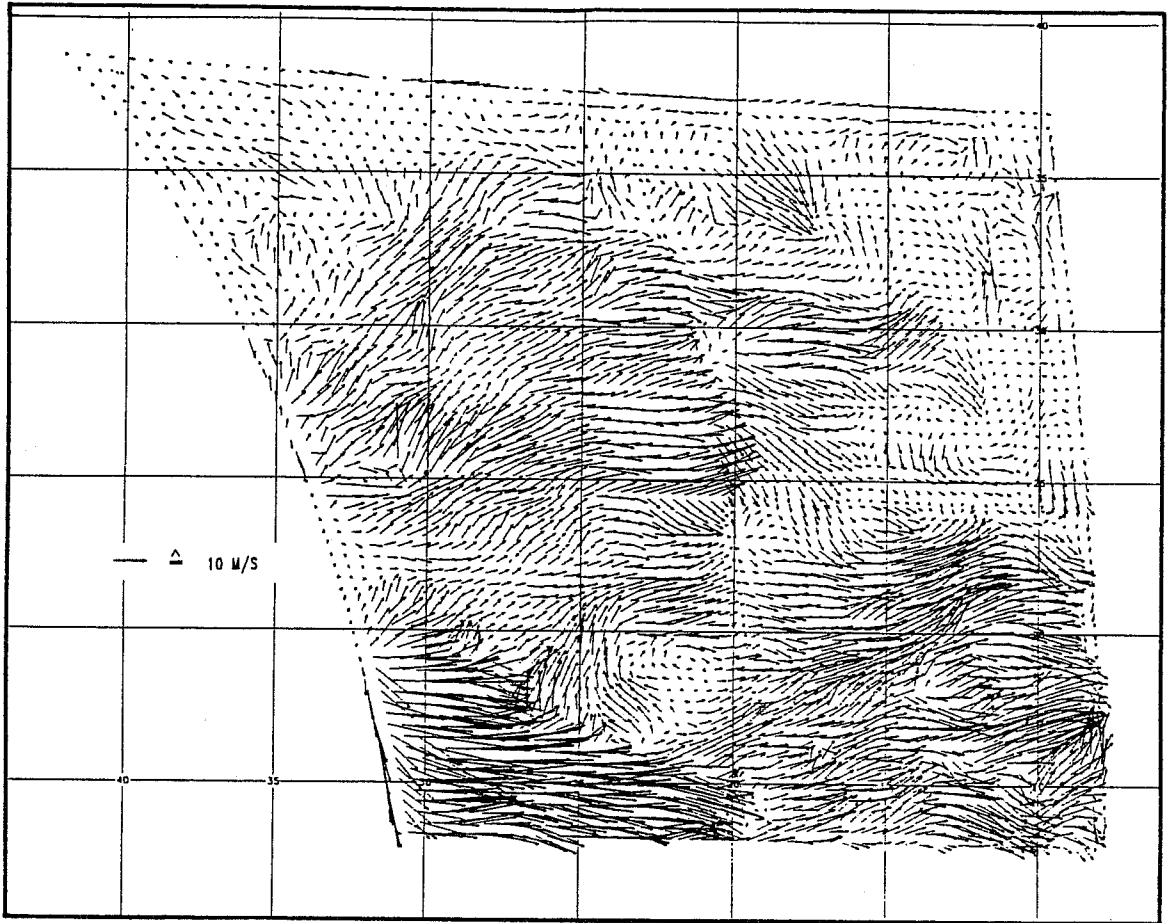


Fig. 6: Case 3: 22 DEC 1988, 22.30-23.00GMT. The center of the image is located at lat=24.4° long=-20.3°. Meteosat3 WV displacement vector field before quality control. The vector field is a composite of four independently computed vector fields from 256\*256 pixels each.



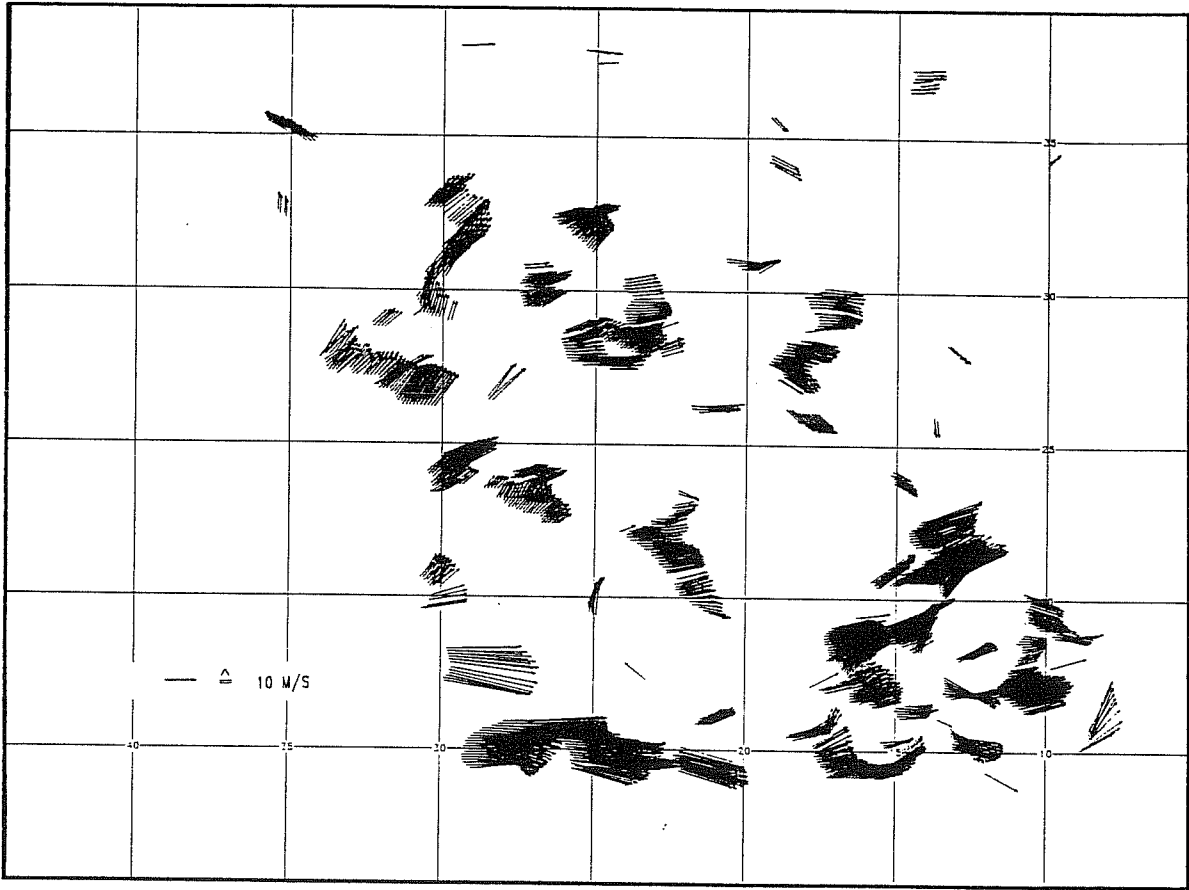


Fig. 7: Same as Fig. 6, but after applying the same consistency checks as in Fig. 3

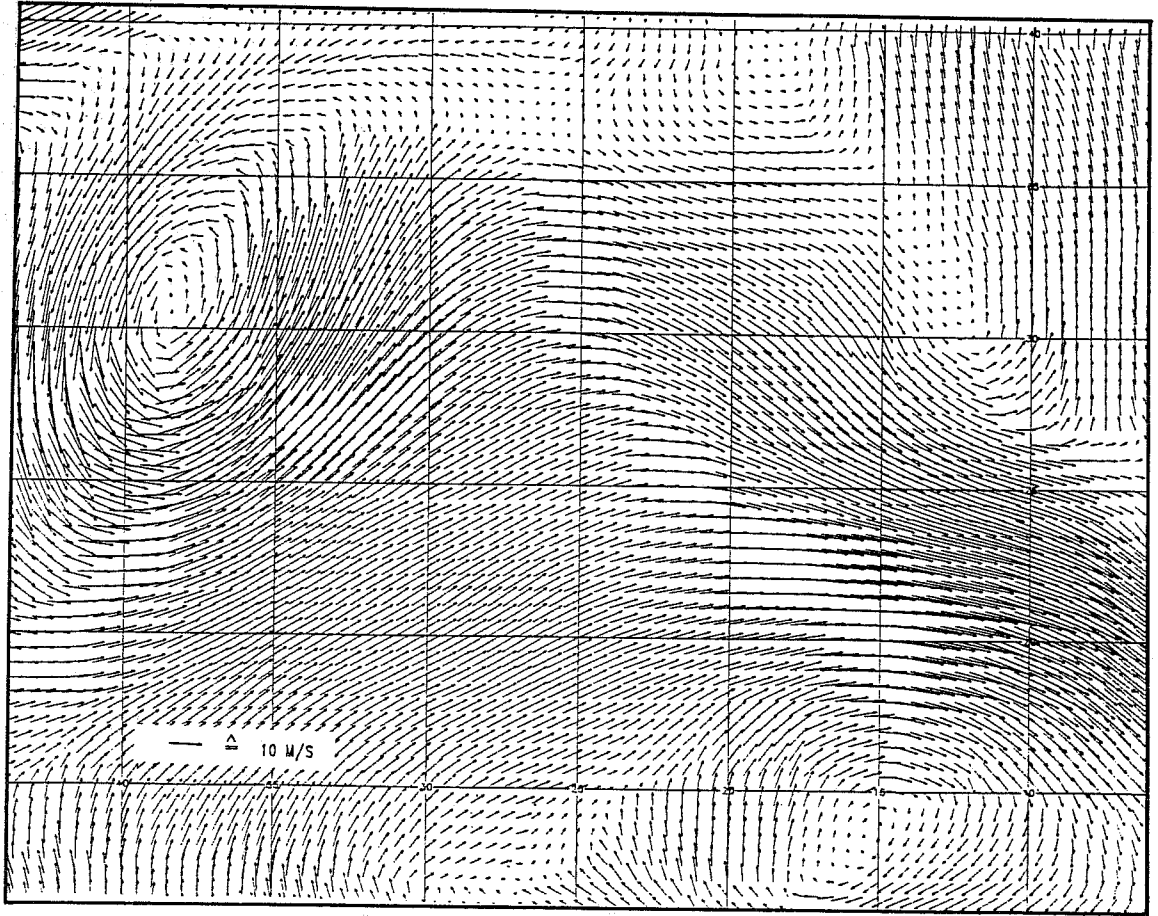


Fig. 8: ECMWF 12-hourly 500hPa forecast for case 3  
22 DEC 1988, 24GMT

	RMS vec. diff. m/s	RMS dir. diff.	RMS speed diff. m/s	cases
GOES high CTW (+) 1979-1982, comp. with RAWIN	10-18	25°-35°	7-15	
METEOSAT 1979 (*) high CTW	12.7	35.0°	10.2	127
700-400hPa CTW comp. with RAWIN	8.7	51.7°	7.0	95
This study:				
Case 1, comp. with interpol. RAWIN 500hPa	9.0	37.2° (23.6°)	5.4 (4.0)	31
Case 3, comp. with 500hPa ECMWF 12-hourly forecast	8.3	36.7° (29.2°)	6.3 (4.4)	3548

Tab. 2: Comparison between CTW and automatically derived WVW displayed in Fig.3 and Fig.7. WVW fields were only subject to an automated internal consistency check, without employing meteorological knowledge. Numbers in brackets denote mean arithmetic differences. (+) from figures in Whitney, 1983  
(\*) Steinhorst, 1979

#### 4. CONCLUSIONS

The high accuracy of water vapour winds, fully comparable to that of cloud track winds, has been demonstrated for interactively single point tracked GOES-VAS winds in the 6.7 $\mu$ m and 7.2 $\mu$ m channels. Since these results were obtained from tracking both WV-structures and high level clouds, it does not make sense from an operational point of view to restrict the selection of targets to pure WV structures, as long as correct height assignment is assured. With the better quality of the METEOSAT3 WV channel, it should be possible to obtain single point tracked WV winds of a similar quality.

Since studies of WV winds have mostly taken place over Europe and the United States, it should be interesting to investigate the quality of WVW in the tropics and subtropics. If good results were obtainable here as well, WVW might be a valuable extra source of information in data sparse regions.

Regarding automated techniques, the nature of the WV channel still yields many problems. A major problem here seems to be the subsequent quality control. Too little knowledge exists about the variety of phenomena tracked and their appropriate height assignment. Studies using single point tracking in a variety of latitudes and synoptical situations should contribute to collecting the knowledge necessary to develop quality control schemes for future automated WWV computation on a sound basis.

#### Acknowledgements

The author expresses her thanks to:

- G. Warnecke, for guidance and helpful suggestions
- Bundesministerium für Forschung und Technologie, for supporting this study under grant 01 QS 1748
- H. Nagel and W. Enkelmann, Fraunhofer Institut, IITB Karlsruhe, for providing the displacement vector algorithm.

#### References

Allison, L.J., Steranka, J., Cherrix, G.T., Hilsenrath, E., 1972: Meteorological applications of the NIMBUS 4 Temperature-Humidity Infrared Radiometer, 6.7 micron channel data. Bull. Americ. Meteor. Soc., 53, 526-535.

Desbois, M., Kayiranga, Th., Gnamien, B., Guessous, S., Picon, L., 1988: Characterization of some elements of the Sahelian climate and their interannual Variations for July 1983, 1984 and 1985 from the analysis of METEOSAT ISCCP data. J. of Climate, 1, 887-904.

Eigenwillig, N., Fischer, H., 1982: Determination of midtropospheric wind vectors by tracking pure water vapor structures in METEOSAT water vapor image sequences. Bull. Americ. Meteor. Soc., 63, No. 1, 44-58.

Enkelmann, W., 1985: Mehrgitterverfahren zur Ermittlung von Verschiebungsvektorfeldern. Thesis, Fachbereich Informatik, Universität Hamburg.

Fischer, H., Eigenwillig, N., Müller, H. 1981: Information content of METEOSAT and NIMBUS/THIR water vapor channel data: Altitude association of observed phenomena. J. Appl. Meteor., 20, 1344-1352.

Fischer, H., Gesell, G., 1987: Abschlußbericht zum DFG-Forschungsvorhaben. Fi 242/9-5.

- Gesell, G., Fischer, H., König, T., 1984: Reduction of noise interference from METEOSAT water vapor image data by means of Fourier Transform and Frequency Domain Filtering. *J. Atmos. Ocean. Technol.*, 1, 147-151.
- Hayden, Ch.M., Stewart, T.R., 1987: An update on cloud and water vapor tracers for providing wind estimates. Proc. 6th Symposium on Meteorological Observations and Instrumentation, Jan. 12-16, New Orleans, La. Published by the American Meteorological Society, Boston, Mass.
- Horn, B.K.P., Schunck, G., 1981: Determining optical flow. *Artificial Intelligence*, 17, 185-203.
- Kästner, M., Fischer, H., Bolle, H.J., 1980: Wind determination from NIMBUS 5 observations in the 6.3  $\mu$ m Water Vapor Band. *J. Appl. Meteor.*, 19, 409-417.
- Morel, P., Desbois, M., Szejwach, G., 1978: A new insight into the troposphere with the water vapor channel of METEOSAT. *Bull. Americ. Meteor. Soc.*, 59, 711-714.
- Nagel, H., 1983a: Displacement vectors derived from second order intensity variations in image sequences. *Computer Vision, Graphics and Image processing*, 21, 85-117.
- Nagel, H., 1983c: Constraints for the estimation of displacement vector fields. Proc. Int. Joint Conference on Artificial Intelligence, Karlsruhe, Aug. 8-12 1983, 945-951.
- Nagel, H., 1985: Analyse und Interpretation von Bildfolgen. *Informatik Spektrum*, 8, 178-200, 312-327.
- Nagel, H., Enkelmann, W., 1983: Iterative estimation of displacement vector fields from TV-frame sequences. *Signal Processing II*, Elsevier Science Publishers B.V. (North Holland), 299-302.
- Poc., M.M., Roulleau, M., Scott, N.A., Chedin, A., 1980: Quantitative studies of METEOSAT water vapor channel data. *J. Appl. Meteor.*, 19, 868-876.
- Steinhorst, G., 1979: METEOSAT cloud winds quality; Report by the German Met. Service. M.O.A.G., ESA-ESOC, Darmstadt.
- Stewart, T.R., Hayden, Ch.M., Smith, W.L., 1985: A note on water vapor wind tracking using VAS data on McIDAS. *Bull. Americ. Meteor. Soc.*, 66, No. 9., 1111-1115.
- Whitney, L.F., 1983: International comparison of satellite winds - An update. *Adv. Space Res.*, 2, 73-77.
- Warnecke, G., 1983: Aspects of dynamic scene analysis in meteorology. In T.S. Huang (ed.): *Image sequence processing and dynamic scene analysis*. 594-600. Springer-Verlag Berlin Heidelberg.